Geophysical Research Letters

RESEARCH LETTER
10.1029/2019GL083596

Interannual Sea Level Variability Along the Southeastern Seaboard of the United States in Relation to the Gyre-Scale Heat Divergence in the North Atlantic

Denis L. Volkov[1,2], Sang-Ki Lee[2], Ricardo Domingues[1,2], Hong Zhang[3], and Marlos Goes[1,2]

[1]Cooperative Institute for Marine and Atmospheric Studies, University of Miami, Miami, FL, USA, [2]Atlantic Oceanographic and Meteorological Laboratory, National Oceanic and Atmospheric Administration, Miami, FL, USA, [3]Joint Institute for Regional Earth System Science and Engineering, University of California, Los Angeles, CA, USA

Abstract The low-amplitude, large-scale, interannual, and longer-term sea level changes are linked to the variations of ocean heat and freshwater content and strongly controlled by ocean dynamics. Near the coast, especially in low-lying and flood-vulnerable regions, these changes can provide background conditions favorable for the occurrence of extreme sea levels that represent a threat for coastal communities and ecosystems. In this study, we identify a tripole mode of the ocean gyre-scale sea surface height variability in the North Atlantic and show that this mode is responsible for most of the interannual-to-decadal sea surface height changes along the southeast coast of the United States, including the Gulf of Mexico. We also show that these changes are largely driven by the large-scale heat divergence related to the Atlantic Meridional Overturning Circulation and linked to the low-frequency North Atlantic Oscillation.

Plain Language Summary The global mean sea level rise caused by ocean warming and terrestrial glacier melting is one of the most alarming aspects of climate change. However, ocean and atmosphere dynamics make sea level change spatially and temporally nonuniform. In fact, the ocean exhibits certain patterns of sea level change with alternating signs over different time periods. These patterns provide background conditions, on top of which shorter-period and often stronger weather-driven sea level fluctuations are superimposed. In order to improve our capacity to predict regional sea level variability, it is important to identify these patterns and to explore the mechanisms responsible for their evolution. In this study, we identify such a pattern in the North Atlantic Ocean and show that it is largely responsible for year-to-year changes of coastal sea level south of Cape Hatteras and in the Gulf of Mexico. These coastal regions of the United States are particularly vulnerable to extreme weather conditions, such as tropical storms and hurricanes, that can cause catastrophic flooding. We show that the temporal evolution of the identified pattern is due to the basin-scale ocean heat content changes in the North Atlantic, driven by changes in the large-scale ocean and atmosphere circulations.

Key Points:
- Interannual sea surface height variability in the North Atlantic exhibits a tripole pattern
- The sea surface height tripole explains up to 60–80% of interannual sea level variance along the southeast U.S. coast and in the Gulf of Mexico
- The tripole is associated with gyre-scale heat divergence in response to low-frequency North Atlantic Oscillation

Supporting Information:
- Supporting Information S1

Correspondence to:
D. L. Volkov,
denis.volkov@noaa.gov

Citation:
Volkov, D. L., Lee, S.-K., Domingues, R., Zhang, H., & Goes, M. (2019). Interannual sea level variability along the southeastern seaboard of the United States in relation to the gyre-scale heat divergence in the North Atlantic. *Geophysical Research Letters*, *46*, 7481–7490. https://doi.org/10.1029/2019GL083596

Received 4 FEB 2019
Accepted 11 JUN 2019
Accepted article online 20 JUN 2019
Published online 1 JUL 2019

1. Introduction

Regional sea level fluctuations occur on a wide range of time scales, from days to decades, with amplitudes much greater than the global mean sea level (GMSL) rise (e.g., Chafik et al., 2019; Holgate & Woodworth, 2004; Meyssignac & Cazenave, 2012; Volkov et al., 2017). Coastal flooding is often caused by short-term (several days) sea level fluctuations due to synoptic changes in atmospheric pressure and wind, often superimposed on spring tide. The low-frequency (periods from months and longer) and large-scale sea level changes provide a background state that can modulate the effect of synoptic and tidal conditions (e.g., Sweet et al., 2018 ; Wdowinski et al., 2016). For instance, in the low-lying southeast coasts of the United States, often hit by tropical storms and hurricanes, the superposition of the background state and synoptic conditions may lead to extreme sea level fluctuations (storm surges) with potentially devastating socioeconomic consequences (e.g., Ezer & Atkinson, 2014). Therefore, in order to develop regional sea level prediction systems and mitigate potential hazards for coastal communities, it is important to first identify the different drivers of sizable sea level changes, such as those associated with large-scale regional

Table 1
Correlation Coefficients Between the Temporal Evolution of the North Atlantic SSH Tripole (EOF_1) and the Low-Pass Filtered (Interannual) and Detrended Tide Gauge Records Shown in Figures 2a and 2b

Tide gauge	Correlation with PC_1
Beaufort (NC)	0.64 (0.73)
Charleston (SC)	**0.84** (0.74)
Fort Pulaski (GA)	**0.76** (0.74)
Trident Pier (FL)	**0.80** (0.65)
Key Virginia (FL)	**0.78** (0.64)
Key West (FL)	**0.82** (0.68)
San Juan (PR)	0.47 (0.48)
St. Petersburg (FL)	**0.64** (0.63)
Pensacola (FL)	**0.72** (0.61)
Grand Isle (LA)	**0.69** (0.59)
Galveston (TX)	**0.82** (0.65)
Port Isabel (TX)	0.53 (0.60)

The 95% significance level (s95) for correlation is shown in brackets (coefficients significant at 95% level are shown in bold font).

patterns, and then investigate the mechanisms of their variability and understand how these patterns translate to coastal sea level change.

The northeast U.S. coast, north of Cape Hatteras, was identified as a "hot spot" for accelerated sea level rise (SLR) in the North Atlantic (NA; Sallenger et al., 2012). Here SLR over the past several decades is significantly higher than the GMSL change (Boon, 2012). A number of local and remote processes were proposed to explain this regional acceleration, such as the effects of longshore wind forcing (Kenigson et al., 2018; Piecuch et al., 2016; Woodworth et al., 2014), atmospheric pressure loading (Piecuch & Ponte, 2015), and weakening of the Gulf Stream and the Atlantic Meridional Overturning Circulation (AMOC; Dong et al., 2019; Ezer, 2015; Goddard et al., 2015; Park & Sweet, 2015; Ezer et al., 2013; Bingham & Hughes, 2009; Levermann et al., 2005). The empirical relationship with the AMOC might not be causal, however, as it can arise from temporally coherent, but spatially separated atmospheric forcing linked to the North Atlantic Oscillation (NAO; Piecuch et al., 2019; Volkov et al., 2019). A modeling study suggests that the AMOC variations are relevant only at interdecadal and longer time scales, while changes in the longshore wind forcing explain the majority of regional sea level variance over shorter time scales (Little et al., 2017). In addition, although the sea level variability is apparently coherent along the NA western boundary on interannual to decadal time scales (Thompson & Mitchum, 2014), a recent study has demonstrated that the region of high coastal SLR rates migrates meridionally, probably resulting from the combined cumulative effect of NAO and El Niño–Southern Oscillation (Valle-Levinson et al., 2017). Specifically, a pronounced acceleration of SLR in 2010–2015 was observed south of Cape Hatteras, while a deceleration occurred north of the cape (Park & Sweet, 2015). The former was recently attributed to warming of the Gulf Stream waters, with some evidence pointing to the associated large-scale changes in the Gulf of Mexico and in the Atlantic Warm Pool (Domingues et al., 2018). The 2010–2015 warming of the Gulf Stream waters is consistent with the large-scale heat convergence in the NA subtropical gyre (Volkov et al., 2019).

In this study, we identify the leading mode of the gyre-scale interannual sea surface height (SSH) variability in the NA, which we term the North Atlantic SSH tripole, and show that this mode is largely responsible for the interannual sea level variations along the U.S. Atlantic coast south of Cape Hatteras and in the Gulf of Mexico. We further discuss how this mode is related to the NA atmospheric circulation and to the AMOC, with a particular focus on the meridional heat divergence across the NA subtropical gyre.

2. Materials and Methods

2.1. Sea Level Measurements

We use the monthly maps of SSH anomaly for the time period from January 1993 to December 2017 distributed by AVISO (www.aviso.altimetry.fr; Pujol et al., 2016). Satellite altimetry data are compared with monthly sea level records at 12 tide gauges located along the southeast coast of the United States (Figure 2 and Table 1). Similar to altimetry, tide gauge records were corrected for the inverted barometer effect (see Text S1 in the supporting information). The linear detrending effectively removes the GMSL rise and glacial isostatic adjustment from the altimetry and tide gauge data. This is because the residual GMSL signal (i.e., linear trend removed) is an order of magnitude smaller than the detrended SSH anomalies, and glacial isostatic adjustment can be assumed linear over the considered time period (Sallenger et al., 2012).

2.2. Temperature and Salinity Fields

To relate the altimetric sea level variability to steric (due to density variations) and thermosteric (due to temperature variations only) processes, we use the monthly gridded profiles of temperature and salinity from January 2004 to December 2017, produced by the Japan Agency for Marine-Earth Science and Technology from all available data including (and mostly) Argo floats (Hosoda et al., 2008). Steric (SSL) and thermosteric (TSL) sea levels are computed by integrating in situ density anomaly (ρ') with respect to the time mean over the upper 1,100 m, which is the depth of the meridional overturning stream function maximum at 26.5°N in the NA (McCarthy et al., 2015; Text S1).

To obtain information on the thermosteric sea level in the Florida Straits, where Argo data are not available, we use temperature profiles from 1,925 eXpendable BathyThermograph (XBT) and 541 Conductivity-Temperature-Depth (CTD) casts in the Florida Current during 1995–2016 (Domingues et al., 2018; Figure S1). Available profiles are averaged over three-month intervals (January–March, April–June, July–September, October–December), and an average annual cycle is computed for the four seasons and subtracted from the data.

2.3. Meridional Heat Transport

To link the observed gyre-scale changes of sea level and heat content to oceanic heat advection, we use the 12-hourly time series of the meridional heat transport (MHT) from April 2004 to February 2017 derived from measurements by the RAPID/MOCHA/WBTS (hereafter RAPID) observing system at 26.5°N (Johns et al., 2011). The MHT time series are averaged monthly, thus yielding 155 monthly estimates. In addition, to extend the estimates of MHT over the full 1993–2017 period and estimate heat divergence in the subtropical NA, we compute the monthly MHT at 26°N (MHT_{26}) and 45°N (MHT_{45}) from an ECCO2 (Estimating Circulation and Climate of the Ocean, phase 2) global eddy-permitting ocean data synthesis (Menemenlis et al., 2005; Volkov et al., 2008, 2010; https://ecco.jpl.nasa.gov; Text S1).

2.4. Atmospheric Data

Sea level changes are related to sea level pressure (SLP) and 10-m wind velocity in 1993–2017 provided by the ECMWF's ERA-Interim re-analysis (Dee et al., 2011; www.ecmwf.int). We also use the monthly station-based NAO index, based on the normalized SLP difference between Lisbon (Portugal) and Reykjavik (Iceland) from the Climate Analysis Section of the National Center for Atmospheric Research (Hurrell et al., 2003; https://climatedataguide.ucar.edu).

2.5. Analysis Methods

The seasonal cycle is estimated by fitting the annual and semiannual harmonics in a least squares sense and removed from all fields and time series. To focus on the interannual variability, the time series were further smoothed with a "Lowess" filter with a 1.5-year cutoff period. The 95% significance level (s95) for correlation is estimated as the 95**th** percentile of correlations (r) between the pairs of 10,000 Monte Carlo simulations of random time series that have the same autocorrelation functions as the original time series (henceforth shown in brackets).

An empirical orthogonal functions (EOF) analysis (von Storch & Zwiers, 1999) is used to identify the leading mode (EOF_1) of the interannual sea level variability in the NA (Figures 1a–1d). The spatial pattern of EOF_1 is represented as a regression map obtained by projecting SSH data onto the standardized (divided by standard deviation) principal component (PC_1) time series. Thus, the regression coefficients are in centimeters (local change of sea level) per 1 standard deviation change of PC_1 (Figure 1d). We then compute the reconstructed SSH fields associated with the first mode: $SSH_{rec}(\boldsymbol{x},\boldsymbol{y},\boldsymbol{t}) = PC_1(\boldsymbol{t}) \times EOF_1(\boldsymbol{x},\boldsymbol{y})$ and the portion of local variance explained by EOF_1: $V_{exp} = 1 - \text{var}(SSH - SSH_{rec})/\text{var}(SSH)$ (Figure 1e).

3. Results

3.1. The North Atlantic SSH Tripole

Volkov et al. (2019) showed that the leading mode (EOF_1) of the interannual sea level variability in the NA in 2004–2016 was characterized by a large-scale tripole pattern. A similar tripole has been known to be the dominant mode of interannual sea surface temperature (SST), linked to multiple forcing mechanisms including the NAO, Atlantic Multidecadal Oscillation, and tropical-extratropical teleconnections (Brown et al., 2016; Deser & Timlin, 1997; Kushnir, 1994; Okumura et al., 2001; Peng et al., 2002; Schneider & Fan, 2012; Wu et al., 2007; Xie & Tanimoto, 1998). Here we show that the NA SSH tripole pattern (or simply the tripole) holds for the entire satellite altimetry record starting from 1993.

The EOF_1 of the low-pass-filtered SSH (Figure 1a) explains 26.7% of the interannual sea level variance, and displays three bands: the subtropical band (stretching from the Caribbean to Europe and including the Gulf Stream and the North Atlantic Current) varies out of phase with both the tropical and the subpolar bands. The EOF_1 of the low-pass-filtered SSL (Figure 1b) in 2004–2017 (Argo period) explains 47.9% of the interannual SSL variance and shows the same tripole pattern. This is expected, because the large-scale interannual

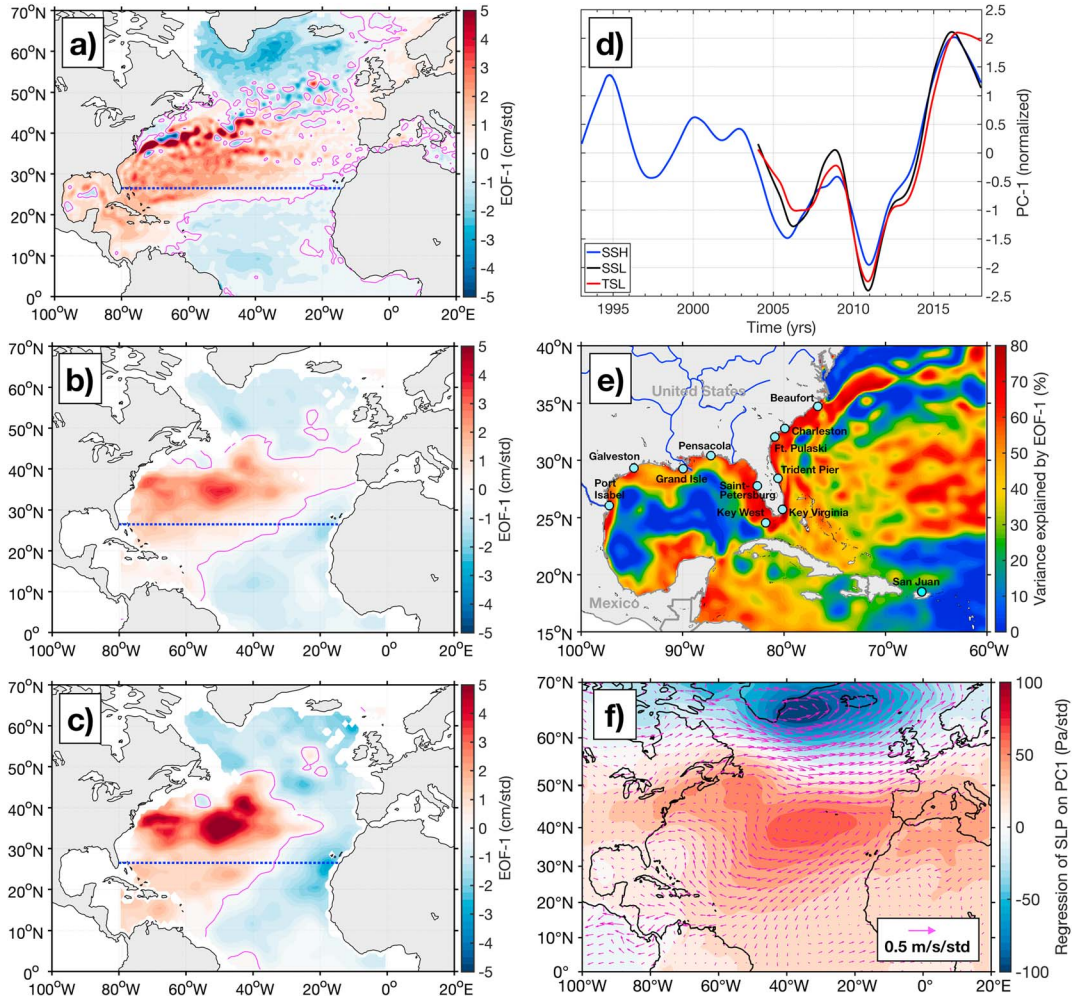

Figure 1. (a–d) The first empirical orthogonal function (EOF_1) of the interannual sea level variability: (a) EOF_1 of SSH explaining 26.7% of the interannual SSH variance; (b) EOF_1 of SSL explaining 47.9% of the interannual SSL variance; (c) EOF_1 of TSL explaining 44.6% of the interannual TSL variance; and (d) temporal evolutions (PC_1) of EOF_1 of (blue) SSH, (black) SSL, and (red) TSL. The approximate location of the RAPID/MOCHA/WBTS observing array is shown by the dotted blue line. (e) Portion of the local interannual SSH variance (%) explained by EOF_1; the location of tide gauges used in the analysis is shown by circles. (f) Regression map of (color) SLP on PC_1 and (arrows) wind velocity on PC_1; the units are Pa per standard deviation of PC_1 and m/s per standard deviation of PC_1, respectively.

sea level variability is mostly steric in nature (e.g.,Chafik et al., 2019 ; Volkov & van Aken, 2003 ; Wunsch et al., 2007). Furthermore, the structure of the tripole is mostly determined by the TSL variability, illustrated by the EOF_1 of the low-pass filtered TSL (Figure 1c). The halosteric component plays a minor role, only partially balancing the thermosteric component (Volkov et al., 2019). The higher percentage of variance explained by the EOF_1 of SSL and TSL (47.9 and 44.6%) compared to the EOF_1 of SSH (26.7%) is presumably due to the differences in the spatial resolution (mesoscale eddies are not present in Argo data) and temporal coverage of Argo and altimetry data.

The temporal evolution (PC_1) of the tripole (Figure 1d) manifests a decadal-scale lowering of sea level and associated heat content from 1993 to 2010 in the subtropical band and the opposite change in the tropical and subpolar bands. Shorter-term interannual fluctuations with periods of about five to seven years are also superimposed on the decadal signal. One of these fluctuations with an extreme (record minimum) value in 2010 coincided with a strongly negative NAO, the upper ocean cooling in the subtropical NA, and a 30% reduction in the AMOC (Bryden et al., 2014; Cunningham et al., 2013; Srokosz & Bryden, 2015). Starting from 2010 to 2016, sea level and heat content increased abruptly in the subtropical band and decreased in the tropical and subpolar bands. This is the period during which an accelerated SLR along the U.S.

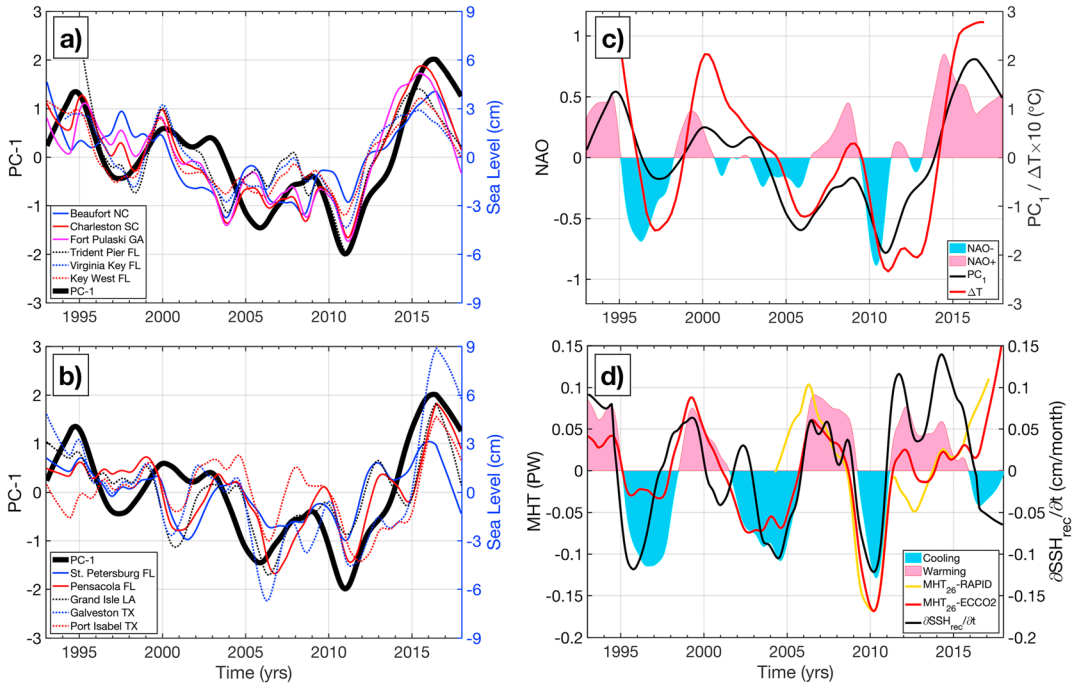

Figure 2. (a and b) PC_1 of the interannual SSH variability (solid black curve) and the low-pass-filtered tide gauge records (solid and dotted curves) along the U.S. southeast coast in (a) the Atlantic Ocean and (b) the Gulf of Mexico. (c) Filled area shows the low-pass-filtered negative (blue) and positive (pink) NAO index, PC_1 (black curve), the low-pass-filtered temperature anomaly averaged over the upper 700 m (scaled by 10 for clarity) in the Florida Straits. (d) The meridional heat transport anomaly (positive northward) computed from (yellow) observations at RAPID/MOCHA/WBTS array (26.5°N), and (red) from ECCO2 model at 26°N, (filled area) the difference between the meridional heat transports at 26°N and at 45°N in ECCO2 (pink/blue means warming/cooling of the subtropical band of the tripole), and the time derivative of SSHrec (cm/month; note that 0.1-PW anomaly in MHT is equivalent to 0.1-cm/month change in thermosteric sea level between 26 and 45°N in the Atlantic).

southeast coast was observed and attributed to the warming of the Florida Current and Gulf Stream (Domingues et al., 2018), associated with the subtropical band.

3.2. Relation to Sea Level Along the Southeast U.S. Coast

It appears that the tripole explains most of the coastal interannual sea level variance (60–80%) south of Cape Hatteras, in the Gulf of Mexico, and in the western Caribbean (Figures 1e and S2). On a broader scale, the tripole explains over 60% of the local sea level variance in the central part of the subtropical band and in the Labrador and Irminger Seas (subpolar band; Figure S2). However, the tripole explains very little coastal sea level variance north of Cape Hatteras, probably due to the dominant role of local atmospheric forcing in driving coastal sea level changes in the region (e.g., Domingues et al., 2018; Piecuch & Ponte, 2015). It should be also noted that the tripole does not explain much variance in the interior of the Gulf of Mexico, in the Gulf Stream, and in the North Atlantic Current north of 40°N, probably due to the dominance of eddy variability in those regions.

South of Cape Hatteras and in the Gulf of Mexico, the temporal evolution of the tripole (PC_1) is well correlated with low-pass-filtered and detrended tide gauge records (Table 1 and Figures 2a and 2b). While other local processes are undoubtedly responsible for higher-frequency fluctuations of sea level at tide gauge locations, the lower frequency interannual-to-decadal changes, such as the lowering of sea level in 1993–2010 and the accelerated SLR in 2011–2015, correspond very well to large-scale changes associated with the tripole. Consistent with the map of explained variance (Figure 1e), the correlations between PC_1 and most tide gauge records are statistically significant (Table 1). The lowest correlation at the edge of significance (0.47) is observed at San Juan (Puerto Rico).

By definition, steric anomalies diminish over the continental shelf as the water column shoals. A steric anomaly over the deep ocean must, therefore, generate a cross-shelf SSH gradient. If there are no forces

present to balance this SSH gradient, it is reasonable to assume that fast barotropic gravity waves immediately distribute this anomaly evenly across the shelf and the deep ocean (Landerer et al., 2007). The SSH gradient can be balanced by the along-shelf geostrophic current, like the Gulf Stream, but it is unclear to what extent this geostrophic adjustment is effective. While a detailed investigation of such mechanism is beyond the scope of this study, observational evidence suggests that a fast barotropic adjustment can be the main mechanism along the southeast U.S. coast, where the Gulf Stream flows close to the shore allowing for steric anomalies to be quickly redistributed. For example, unprecedented warming of the Florida Current in 2010–2015 did account for most of coastal SLR south of Cape Hatteras, but not further north, where the Gulf Stream detaches from the coast (Domingues et al., 2018).

3.3. Relation to Atmospheric Forcing

The low-pass-filtered SLP and 10-m wind velocity were regressed on PC_1 to relate the NA SSH tripole to atmospheric forcing. The obtained atmospheric circulation pattern displays a dipole structure similar to the NAO pattern (Figure 1f). The positive/negative anomalies of PC_1 (Figure 1d), associated with a higher/lower sea level in the subtropical band and lower/higher sea levels in the tropical and subpolar bands (Figure 1a), correspond to stronger/weaker subtropical high and subpolar low SLP centers and to stronger/weaker westerly winds in the midlatitude NA (40°N–60°N) and trade winds (10°N–30°N). The maximum correlation between PC_1 and NAO index is 0.76 (s95 = 0.51) when the former lags the latter by nine months (Figure 2c). The positive/negative NAO indices are associated with the nine-month lagged rising/lowering sea level in the subtropical band and lowering/rising sea level in the tropical and subpolar bands.

It is noted that maximum sea level fluctuations in the subtropical band are concentrated in the western part of the basin (Figure 1a), and are not collocated with the maximum NAO-modulated SLP changes centered near the Mid-Atlantic Ridge (Figure 1f). This suggests that the tripole is not simply a reflection of Ekman pumping and deepening/shoaling of isopycnals in the subtropical gyre caused by the NAO but also results from the adjustment of the large-scale horizontal and overturning ocean circulation to variable surface buoyancy and wind forcing (Marshall et al., 2001; Visbeck et al., 2013; Williams et al., 2014). It should also be noted that the NA SSH tripole is highly correlated with the NA SST tripole (Xie & Tanimoto, 1998), suggesting that both are subject to the same forcing mechanisms. The relationship between the NA SST tripole and SSH tripole is shown and further discussed in Text S1 and Figure S3 (Reynolds et al., 2002).

Near-shore winds, associated with the large-scale and low-frequency NAO pattern, can also affect coastal sea level (e.g., Piecuch et al., 2016, 2019; Woodworth et al., 2014). As illustrated in Figure 1f, rather strong (up to 0.3 m/s per 1 standard deviation of PC_1) and predominantly easterly wind anomalies occur in the vicinity of Cape Hatteras. South of Cape Hatteras the alongshore wind influence on the 2010–2015 SLR was generally below 25% (Domingues et al., 2018). However, it is quite difficult to cleanly separate the influences of the alongshore winds and ocean warming on the SSH variability. This is because local winds are correlated with the large-scale atmospheric forcing, modulated by NAO, which also drives the oceanic heat divergence. Therefore, wind-induced coastal sea level changes are also correlated with the tripole.

3.4. Relation to Ocean Heat Divergence

The Gulf Stream waters warmed by about 1 °C in 2010–2015 and caused the accelerated SLR south of Cape Hatteras (Domingues et al., 2018). Here we use the same multiyear observing network composed of XBT and CTD transects in the Florida Straits (Figure S1) to relate local ocean temperature changes to the NA SSH tripole. The time series of the low-pass-filtered temperature anomaly averaged in the Florida Straits over the upper 700 m in 1995–2017 is well correlated ($\boldsymbol{r} = 0.75$ at s95 = 0.68) with PC_1 (Figure 2c, red and black curves, respectively): higher/lower sea level in the subtropical band of the tripole is associated with the warmer/colder Florida Current. This comparison not only complements the results obtained from Argo data about the thermosteric nature of the tripole (Figure 1c) but also extends these results closer to the U.S. east coast, to the depths where Argo data (usually restricted by 2,000-m isobath) are not available. This suggests that thermal anomalies in the Florida Current may dominate the interannual sea level variability along the U.S. southeast coast over the entire observational period.

In addition to the correlation with the low-frequency NAO-modulated atmospheric circulation, the NA SSH tripole is driven by changes in the large-scale ocean circulation, which is often represented by the AMOC.

The RAPID observing array lies approximately along the boundary between the subtropical and tropical bands of the tripole (Figures 1a–1c), and MHT estimates across this array can be indicative of heat divergence in these two bands (Volkov et al., 2019). It should be noted that correlation between MHT and AMOC at 26.5°N exceeds 0.9 (Johns et al., 2011;Text S1). The detrended low-pass-filtered MHT time series obtained from the RAPID array and from the ECCO2 model at 26°N (MHT_{26}) in 2004–2017 agree well (Figure 2d), suggesting that the model is likely to reproduce the MHT prior to 2004. Both PC_1 and temperature anomaly in the Florida Straits follow changes in MHT_{26} (Figures 2c and 2d). The maximum correlation between PC_1 and MHT_{26} in 1993–2017 is 0.65 (s95 = 0.57) at one-year time lag. It should be remembered that sea level response (PC_1) is proportional to the time integral of heat advection, which is the reason for the observed time lag between MHT_{26} and PC_1.

Because the ECCO2 model adequately simulates MHT at 26°N, we assume that it is also robust at other latitudes and thus compute the difference between MHT_{26} and MHT_{45}, which is a good proxy for heat divergence in the subtropical band of the tripole ($\Delta MHT = MHT_{26} - MHT_{45}$). Positive/negative differences lead to warming/cooling and increase/decrease of sea level (Figure 2d). The time change of SSH due to the net advective heat divergence is given by $\partial SSH/\partial t = \alpha\ \Delta MHT\ (\rho C_p A)^{-1}$, where $\boldsymbol{\alpha}$ is the thermal expansion coefficient, $\boldsymbol{\rho}$ is the density, $\boldsymbol{C_p}$ is the specific heat capacity of seawater, and $\boldsymbol{A}$ is the ocean area. With the typical values of $\boldsymbol{\alpha} = 2 \times 10^{-4}$ °C, $\boldsymbol{\rho} = 1{,}025$ kg/m^3, $\boldsymbol{C_p} = 3{,}990$ J kg^{-1} °C^{-1}, and $\boldsymbol{A} = 1.3 \times 10^{13}$ m^2, the net heat advection of $\Delta MHT = 0.1$ PW (1 PW = 10^{15} W) over one-month time interval is equivalent to the area-averaged $\partial SSH/\partial \boldsymbol{t} = 0.1$ cm/month. The time series of ΔMHT and, hence, associated $\partial SSH/\partial \boldsymbol{t}$ (driven by heat advection) in the model (shaded area in Figure 2d) are well correlated ($\boldsymbol{r} = 0.78$ at s95 = 0.5) and of the same magnitude with the time change of altimetry SSH reconstructed with EOF_1 ($\partial SSH_{rec}/\partial \boldsymbol{t}$; see section 2.5) and averaged between 26°N and 45°N in the NA (black curve in Figure 2d). This comparison provides a quantitative link between heat divergence and large-scale sea level changes. The differences between ΔMHT and $\partial SSH_{rec}/\partial \boldsymbol{t}$ are mainly due to surface buoyancy fluxes, advection of freshwater, higher modes of variability, and errors in the model and data.

Similar to the tripole, heat divergence between 26°N and 45°N is also related to the low-pass-filtered NAO with a correlation of 0.77 (compare Figures 2c and 2d). The maximum correlation between the MHT at 26°N and NAO is 0.75, when the former leads the latter by four months. This time lag, however, may not be significant for the time series filtered with a 1.5-year window. In addition, because ocean and atmosphere constitute a coupled system, this lead-lag relationship does not necessarily mean that MHT at 26°N drives the NAO. Nevertheless, it highlights the importance of possible oceanic feedback on atmospheric processes. Several earlier studies have shown that SST modulated by the tripole can feedback on to the atmosphere aloft and thus are able to modulate the atmospheric variability over the NA (e.g.,Lee et al., 2016 ; Mo et al., 2009 ; Sutton & Hodson, 2007 ; Wang et al., 2008 ; Weaver et al., 2009 ; Yamamoto & Palter, 2016).

4. Conclusions

In this study, we report that the leading mode of the interannual sea level variability in the NA represents a tripole with the subtropical band varying out of phase with the tropical and subpolar bands (Figure 1a). We demonstrate that over the (rather short) 1993–2017 observational period the tripole explains up to 60–80% of the interannual coastal sea level variance south of Cape Hatteras and in the Gulf of Mexico (Figure 1e); both regions associated with the subtropical band. The temporal evolution of the tripole is significantly correlated with low-pass-filtered tide gauge records in the region, suggesting the relevance of large-scale processes to coastal sea level changes (Figures 2a and 2b). In situ observations indicate that the tripole sea level changes, including sea level changes in the Florida Straits, are mostly thermosteric in nature (Figure 1c). The mean temperature of the Florida Current is well correlated with the temporal evolution of the tripole, suggesting that the Florida Current may serve as an important indicator for the large-scale heat content and associated thermosteric sea level changes in the subtropical NA (Figure 2c).

We show that the tripole SSH variability in the subtropical band of the NA is largely due to the meridional heat divergence influenced by the AMOC (Figure 2d). MHT at 26.5°N appears to be representative of heat exchange between the tropical and subtropical bands of the tripole: a stronger/weaker MHT favors higher/lower thermosteric sea level in the subtropical band, including the southeast U.S. coast, one year later. Consistent with Domingues et al. (2018) and Valle-Levinson et al. (2017), the tripole is also related

to the NAO-controlled low-frequency atmospheric circulation: positive/negative NAO pattern is followed by a higher/lower sea level in the subtropical band with a time lag of nine months (Figure 2c).

Earlier studies have mainly considered the likely connection between the AMOC and sea level along the U.S. eastern seaboard via changes in the Gulf Stream transport (Ezer, 2016; Ezer et al., 2013; Park & Sweet, 2015). Our study represents a somewhat different, but complementary process, in which the coastal sea level is associated with the basin-wide SSH pattern largely controlled by the AMOC-driven divergence of heat and the low-frequency NAO. Because this mechanism is more effective at large spatial (ocean-gyre) and long temporal (interannual and longer) scales, and sea level is proportional to the time integral of oceanic transports, there is a potential for multiyear predictability of sea level using the ocean heat transport at the RAPID/MOCHA/WBTS section. This study is one of the first attempts to link the AMOC observed at 26.5°N to large-scale and coastal sea level variations. The relationships reported here need to be revisited as more observations become available.

Acknowledgments
This work was supported by the NOAA/AOML and by the NASA Ocean Surface Topography Science Team program (via grants NNX13AO73G and NNX17AH59G). Several authors were also supported under the auspices of the Cooperative Institute of Marine and Atmospheric Studies (CIMAS) of the University of Miami and NOAA, cooperative agreement NA10OAR4320143. The authors thank two anonymous reviewers and the Editor for their time and efforts to evaluate this manuscript. The tide gauge data were obtained from the Permanent Service for Mean Sea Level (www.psmsl.org). The Argo data were collected and made freely available by the International Argo Program and the national programs that contribute to it. The JAMSTEC temperature and salinity fields were downloaded from http://www.jamstec.go.jp/ARGO/argo_web/argo/?lang=en. Heat transport for the RAPID/MOCHA/WBTS array was obtained from www.rsmas.miami.edu/users/mocha. Hydrographic data in the Florida Straits are available from NOAA's Atlantic Oceanographic and Meteorological Laboratory (http://www.aoml.noaa.gov/phod/index.php).

References

Bingham, R., & Hughes, C. W. (2009). Signature of the Atlantic meridional overturning circulation in sea level along the east coast of North America. *Geophysical Research Letters*, *36*, L02603. https://doi.org/10.1029/2008GL036215

Boon, J. D. (2012). Evidence of sea level acceleration at US and Canadian tide stations, Atlantic Coast, North America. *Journal of Coastal Research*, *28*, 1437–1445.

Brown, P. T., Lozier, M. S., Zhang, R., & Li, W. (2016). The necessity of cloud feedback for a basin-scale Atlantic Multidecadal Oscillation. *Geophysical Research Letters*, *43*, 3955–3963. https://doi.org/10.1002/2016GL068303

Bryden, H. L., King, B. A., McCarthy, G. D., & McDonagh, E. L. (2014). Impact of a 30% reduction in Atlantic meridional overturning during 2009–2010. *Ocean Science*, *10*(4), 683–691. https://doi.org/10.5194/os-10-683-2014

Chafik, L., Nilsen, J. E. O., Dangerdorf, S., Reverdin, G., & Frederikse, T. (2019). North Atlantic Ocean circulation and decadal sea level change during the altimetry era. *Scientific Reports*, *9*(1), 1041. https://doi.org/10.1038/s41598-018-37603-6

Cunningham, S. A., Roberts, C. D., Frajka-Williams, E., Johns, W. E., Hobbs, W., Palmer, M. D., et al. (2013). Atlantic Meridional Overturning Circulation slowdown cooled the subtropical ocean. *Geophysical Research Letters*, *40*, 6202–6207. https://doi.org/10.1002/2013GL058464

Dee, D. P., Uppala, S. M., Simmons, A. J., Berrisford, P., Poli, P., Kobayashi, S., et al. (2011). The ERA-Interim reanalysis: Configuration and performance of the data assimilation system. *Quarterly Journal of the Royal Meteorological Society*, *137*(656), 553–597. https://doi.org/10.1002/qj.828

Deser, C., & Timlin, M. S. (1997). Atmosphere–ocean interaction on weekly timescales in the North Atlantic and Pacific. *Journal of Climate*, *10*(3), 393–408. https://doi.org/10.1175/1520-0442(1997)010<0393:AOIOWT>2.0.CO;2

Domingues, R., Goni, G., Baringer, M., & Volkov, D. (2018). What caused the accelerated sea level changes along the U.S. East Coast during 2010–2015? *Geophysical Research Letters*, *45*, 13,367–13,376. https://doi.org/10.1029/2018GL081183

Dong, S., Baringer, M., & Goni, G. (2019). Slow down of the Gulf Stream during 1993–2016. *Scientific Reports*, *9*(1), 6672. https://doi.org/10.1038/s41598-019-42820-8

Ezer, T. (2015). Detecting changes in the transport of the Gulf Stream and the Atlantic overturning circulation from coastal sea level data: The extreme decline in 2009–2010 and estimated variations for 1935–2012, Global Planet. *Change*, *129*, 23–36. https://doi.org/10.1016/j.gloplacha.2015.03.002

Ezer, T. (2016). Can the Gulf Stream induce coherent short-term fluctuations in sea level along the US East Coast? A modeling study. *Ocean Dynamics*, *66*(2), 207–220. https://doi.org/10.1007/s10236-016-0928-0

Ezer, T., & Atkinson, L. P. (2014). Accelerated flooding along the U.S. East Coast: On the impact of sea-level rise, tides, storms, the Gulf Stream, and the North Atlantic Oscillations. *Earth's Future*, *2*(8), 362–382. https://doi.org/10.1002/2014EF000252

Ezer, T., Atkinson, L. P., Corlett, W. B., & Blanco, J. L. (2013). Gulf Stream's induced sea level rise and variability along the US mid-Atlantic coast. *Journal of Geophysical Research: Oceans*, *118*, 685–697. https://doi.org/10.1002/jgrc.20091

Goddard, P. B., Yin, J., Griffies, S. M., & Zhang, S. (2015). An extreme event of sea-level rise along the Northeast coast of North America in 2009–2010. *Nature Communications*, *6*(1). https://doi.org/10.1038/ncomms7346

Holgate, S. J., & Woodworth, P. L. (2004). Evidence for enhanced coastal sea level rise during the 1990s. *Geophysical Research Letters*, *31*, L07305. https://doi.org/10.1029/2004GL019626

Hosoda, S., Ohira, T., & Nakamura, T. (2008). A monthly mean dataset of global oceanic temperature and salinity derived from Argo float observations. *JAMSTEC Report of Research and Development*, *8*, 47–59.

Hurrell, J. W., Kushnir, Y., Ottersen, G., & Visbeck, M. (2003). *The North Atlantic Oscillation: Climate significance and environmental impact*, *Geophysical Monograph*, (Vol. 134). American Geophysical Union. https://doi.org/10.1029/GM134

Johns, W. E., Baringer, M. O., Beal, L. M., Cunningham, S. A., Kanzow, T., Bryden, H. L., et al. (2011). Continuous, array-based estimates of Atlantic Ocean heat transport at 26.5°N. *Journal of Climate*, *24*(10), 2429–2449. https://doi.org/10.1175/2010JCLI3997.1

Kenigson, J. S., Han, W., Rajagopalan, B., Yanto, & Jasinski, M. (2018). Decadal shift of NAO-linked interannual sea level variability along the U.S. northeast coast. *Journal of Climate*, *31*(13), 4981–4989. https://doi.org/10.1175/JCLI-D-17-0403.1

Kushnir, Y. (1994). Interdecadal variations in North Atlantic sea surface temperature and associated atmospheric conditions. *Journal of Climate*, *7*(1), 141–157. https://doi.org/10.1175/1520-0442(1994)007<0141:IVINAS>2.0.CO;2

Landerer, F. W., Jungclaus, J. H., & Marotzke, J. (2007). Ocean bottom pressure changes lead to a decreasing length-of-day in a warming climate. *Geophysical Research Letters*, *34*, L06307. https://doi.org/10.1029/2006GL029106

Lee, S.-K., Wittenberg, A. T., Enfield, D. B., Weaver, S. J., Wang, C., & Atlas, R. (2016). U.S. regional tornado outbreaks and their links to ENSO flavors and North Atlantic SST variability. *Environmental Research Letters*, *11*. https://doi.org/10.1088/1748-9326/11/4/044008

Levermann, A., Griesel, A., Hofmann, M., Montoya, M., & Rahmstorf, S. (2005). Dynamic sea level changes following changes in the thermohaline circulation. *Climate Dynamics*, *24*(4), 347–354. https://doi.org/10.1007/s00382-004-0505-y

Little, C. M., Piecuch, C. G., & Ponte, R. M. (2017). On the relationship between the meridional overturning circulation, alongshore winds stress, and United States Coast sea level in the Community Earth System Model Large Ensemble. *Journal of Geophysical Research: Oceans*, *122*, 4554–4568. https://doi.org/10.1002/2017JC012713

Marshall, J., Johnson, H., & Goodman, J. (2001). A study of the interaction of the North Atlantic Oscillation with ocean circulation. *Journal of Climate*, *14*(7), 1399–1421. https://doi.org/10.1175/1520-0442(2001)014<1399:ASOTIO>2.0.CO;2

McCarthy, G. D., Smeed, D. A., Johns, W. E., Frajka-Williams, E., Moat, B. I., Rayner, D., et al. (2015). Measuring the Atlantic Meridional Overturning Circulation at 26°N. *Progress in Oceanography*, *130*, 91–111. https://doi.org/10.1016/jpocean.2014.10.006

Menemenlis, D., Hill, C., Adcrocft, A., Campin, J. M., Cheng, B., Ciotti, B., et al. (2005). NASA supercomputer improves prospects for ocean climate research. *Eos, Transactions American Geophysical Union*, *86*(9), 89–96. https://doi.org/10.1029/2005EO090002

Meyssignac, B., & Cazenave, A. (2012). Sea level: A review of present-day and recent-past changes and variability. *Journal of Geodynamics*, *58*, 96–109. https://doi.org/10.1016/j.jog.2012.03.005

Mo, K. C., Schemm, J.-K. E., & Yoo, S.-H. (2009). Influence of ENSO and the Atlantic Multidecadal Oscillation on drought over the United States. *Journal of Climate*, *22*(22), 5962–5982. https://doi.org/10.1175/2009JCLI2966.1

Okumura, Y., Xie, S.-P., Numaguti, A., & Tanimoto, Y. (2001). Tropical Atlantic air–sea interaction and its influence on the NAO. *Geophysical Research Letters*, *28*(8), 1507–1510. https://doi.org/10.1029/2000GL012565

Park, J., & Sweet, W. (2015). Accelerated sea level rise and Florida Current transport. *Ocean Science*, *11*(4), 607–615. https://doi.org/10.5194/os-11-607-2015

Peng, S., Robinson, W. A., & Li, S. (2002). North Atlantic SST forcing of the NAO and relationships with intrinsic hemispheric variability. *Geophysical Research Letters*, *29*(8), 1276. https://doi.org/10.1029/2001GL014043

Piecuch, C. G., Dangendorf, S., Gawarkiewicz, G. G., Little, C. M., Ponte, R. M., & Yang, J. (2019). How is New England coastal sea level related to the Atlantic meridional overturning circulation at 26°N? *Geophysical Research Letters*, *46*. https://doi.org/10.1029/2019GL083073

Piecuch, C. G., Dangendorf, S., Ponte, R. M., & Marcos, M. (2016). Annual sea level changes on the North American Northeast Coast: Influence of local winds and barotropic motions. *Journal of Climate*, *29*(13), 4801–4816. https://doi.org/10.1175/JCLI-D-16-0048.1

Piecuch, C. G., & Ponte, R. M. (2015). Inverted barometer contributions to recent sea level changes along the northeast coast of North America. *Geophysical Research Letters*, *42*, 5918–5925. https://doi.org/10.1002/2015GL064580

Pujol, M.-I., Faugère, Y., Taburet, G., Dupuy, S., Pelloquin, C., Ablain, M., & Picot, N. (2016). DUACS DT2014: The new multi-mission altimeter data set reprocessed over 20 years. *Ocean Science*, *12*(5), 1067–1090. https://doi.org/10.5194/os-12-1067-2016

Reynolds, R. W., Rayner, N. A., Smith, T. M., Stokes, D. C., & Wang, W. (2002). An improved in situ and satellite SST analysis for climate. *Journal of Climate*, *15*(13), 1609–1625. https://doi.org/10.1175/1520-0442(2002)015<1609:AIISAS>2.0.CO;2

Sallenger, A. H. Jr., Doran, K. S., & Howd, P. A. (2012). Hotspot of accelerated sea-level rise on the Atlantic coast of North America. *Nature Climate Change*, *2*(12), 884–888. https://doi.org/10.1038/nclimate1597

Schneider, E. K., & Fan, M. (2012). Observed decadal North Atlantic tripole SST variability: II. Diagnosis of mechanisms. *Journal of the Atmospheric Sciences*, *69*(1), 51–64. https://doi.org/10.1175/JAS-D-11-019.1

Srokosz, M., & Bryden, H. L. (2015). Observing the Atlantic Meridional Overturning Circulation yields a decade of inevitable surprises. *Science*, *348*(6241). https://doi.org/10.1126/science.1255575

von Storch, H., & Zwiers, F. W. (1999). *Statistical analysis in climate research*, (p. 484). Cambridge University Press.

Sutton, R. T., & Hodson, D. L. R. (2007). Climate response to basin-scale warming and cooling of the North Atlantic Ocean. *J. Clim.*, *20*(5), 891–907. https://doi.org/10.1175/JCLI4038.1

Sweet, W., Dusek, G., Obeysekera, J., and Marra, J. (2018), Patterns and projections of high tide flooding along the U.S. coastline using a common impact threshold. NOAA Technical Report NOS CO-OPS, Vol. 86, National Oceanic and Atmospheric Administration, Silver Spring, 395 Maryland, USA.

Thompson, P. R., & Mitchum, G. T. (2014). Coherent sea level variability on the North Atlantic western boundary. *Journal of Geophysical Research: Oceans*, *119*, 5676–5689. https://doi.org/10.1002/2014JC009999

Valle-Levinson, A., Dutton, A., & Martin, J. B. (2017). Spatial and temporal variability of sea level rise hot spots over the eastern United States. *Geophysical Research Letters*, *44*, 7876–7882. https://doi.org/10.1002/2017GL073926

Visbeck, M., Chassignet, E. P., Curry, R. G., Delworth, T. L., Dickson, R. R., & Krahmann, G. (2013). The ocean's response to North Atlantic Oscillation variability. In J. W. Hurrell, Y. Kushnir, G. Ottersen, & M. Visbeck (Eds.), *The North Atlantic Oscillation: Climatic significance and environmental impact* 113–145. https://doi.org/10.1029/134GM06

Volkov, D. L., Baringer, M., Smeed, D., Johns, W., & Landerer, F. W. (2019). Teleconnection between the Atlantic Meridional Overturning Circulation and sea level in the Mediterranean Sea. *Journal of Climate*, *32*(3), 935–955. https://doi.org/10.1175/JCLI-D-18-0474.1

Volkov, D. L., Fu, L.-L., & Lee, T. (2010). Mechanisms of the meridional heat transport in the Southern Ocean. *Ocean Dynamics*, *60*(4), 791–801. https://doi.org/10.1007/s10236-010-0288-0

Volkov, D. L., Lee, S.-K., Landerer, F. W., & Lumpkin, R. (2017). Decade-long deep-ocean warming detected in the subtropical South Pacific. *Geophysical Research Letters*, *44*, 927–936. https://doi.org/10.1002/2016GL071661

Volkov, D. L., Lee, T., & Fu, L.-L. (2008). Eddy-induced meridional heat transport in the ocean. *Geophysical Research Letters*, *35*, L20601. https://doi.org/10.1029/2008GL035490

Volkov, D. L., & van Aken, H. M. (2003). Annual and interannual variability of sea level in the northern North Atlantic Ocean. *Journal of Geophysical Research*, *108*(C6), 3204. https://doi.org/10.1029/2002JC001459

Wang, C., Lee, S.-K., & Enfield, D. B. (2008). Climate response to anomalously large and small Atlantic warm pools during the summer. *Journal of Climate*, *21*(11), 2437–2450. https://doi.org/10.1175/2007JCLI2029.1

Wdowinski, S., Bray, R., Kirtman, B. P., & Wu, Z. (2016). Increasing flooding hazard in coastal communities due to rising sea level: Case study of Miami Beach. *Florida, Ocean Coastal Manage*, *126*, 1–8. https://doi.org/10.1016/j.ocecoaman.2016.03.002

Weaver, S. J., Schubert, S., & Wang, H. (2009). Warm season variations in the low-level circulation and precipitation over the central United States in observations, AMIP simulations, and idealized SST experiments. *Journal of Climate*, *22*(20), 5401–5420. https://doi.org/10.1175/2009JCLI2984.1

Williams, R. G., Roussenov, V., Smith, D., & Lozier, M. S. (2014). Decadal evolution of ocean thermal anomalies in the North Atlantic: The effects of Ekman, overturning, and horizontal transport. *Journal of Climate*, *27*(2), 698–719. https://doi.org/10.1175/JCLI-D-12-00234.1

Woodworth, P. L., Maqueda, M. Á. M., Roussenov, V. M., Williams, R. G., & Hughes, C. W. (2014). Mean sea-level variability along the northeast American Atlantic coast and the roles of the wind and the overturning circulation. *Journal of Geophysical Research: Oceans*, *119*, 8916–8935. https://doi.org/10.1002/2014JC010520

Wu, L., He, F., Liu, Z., & Li, C. (2007). Atmospheric teleconnections of tropical Atlantic variability: Interhemispheric, tropical–extratropical, and cross-basin interactions. *Journal of Climate*, *20*(5), 856–870. https://doi.org/10.1175/JCLI4019.1

Wunsch, C., Ponte, R. M., & Heimbach, P. (2007). Decadal trends in sea level patterns: 1993–2004. *Journal of Climate*, *20*(24), 5889–5911. https://doi.org/10.1175/2007JCLI1840.1

Xie, S.-P., & Tanimoto, Y. (1998). A pan-Atlantic decadal climate oscillation. *Geophysical Research Letters*, *25*(12), 2185–2188. https://doi.org/10.1029/98GL01525

Yamamoto, A., & Palter, J. B. (2016). The absence of an Atlantic imprint on the multidecadal variability of wintertime European temperature. *Nature Communications*, *7*(1). https://doi.org/10.1038/ncomms10930